Journal of Materials Science: Materials in Electronics (2019) 30:18297–18305
https://doi.org/10.1007/s10854-019-02145-8

Preparation of polyarylene ether nitriles/fullerene composites with low dielectric constant by cosolvent evaporation

Xiting Lei[1] · Lifen Tong[1] · Hai Pan[1] · Guangyao Yang[1] · Xiaobo Liu[1]

Received: 4 June 2019 / Accepted: 3 September 2019 / Published online: 10 October 2019

Abstract
Fullerenes are widely used to reduce the dielectric constant of composites due to their special hollow cage structure. However, the main challenge for the realization of its material potential application is to improve the interfacial compatibility between the polymer matrix and fullerenes. Here we report a pure physical method of cosolvent evaporation to prepare polyarylene ether nitriles (PEN) composite films with well-defined monodisperse clusters of fullerenes for manufacturing flexible printed circuit boards. The presence of fullerenes is proven to be crucial to decrease the dielectric constant of composite films. The film with 3 wt% fullerenes loading possesses the lowest dielectric constant of 2.65 at 1 MHz, and its service life is detected as 3.3 years by Flynn–Wall–Ozawa method. Additionally, when the composite films used in flexible copper clad laminate (FCCL), the 180° peeling strength between the resin and copper foil is 6.91 N cm^{-1}. Therefore, this PEN/fullerene composite provides potential application for the preparation of FCCL.

1 Introduction

Printed Circuit Board (PCB), as a support for electronic components, is a platform for ensuring electrical connection of different functional modules. With the development of advanced microelectronics, new requirements (flexibility, twistability, non-adhesive, etc.) have been placed on PCBs, causing the replacement of rigid PCB to flexible PCB (FPCBs) [1–3]. Much work has been reported in last decade on polyetheretherketone (PEEK) based micro- and nanocomposites containing Al_2O_3 [4], AlN [5], SiO_2 [6], BN [7] particles (both micro and nano) etc. for PCBs. Flexible copper clad laminate (FCCL) which is uniformly consists of a conductive layer and an insulating layer is a main material of FPCBs in practical applications [8–12]. In the context of 5G, some of METIS overall technical goals include 1000 times higher mobile data volume per area and 10 to 100 times higher than typical used data rate relative to today [13], posing the biggest problem to reduce the dielectric constant in order to speed up signal transmission [14–18]. Thus, FCCL with excellent thermal performance, adhesion to copper and low dielectric constant is more suitable for industries.

According to Debye equation [Eq (1)], decreasing the density of film or the polarizability of atoms and chemical bonds can lower the dielectric constant:

$$\frac{k-1}{k+2} = \frac{4\pi}{3}N\left(\alpha_e + \alpha_d + \frac{\mu}{3k_bT}\right) \quad (1)$$

where N is the number density of dipoles, α_e is the electronic polarization, α_d is the distortion polarization, $\mu/3k_bT$ is orientation polarization related to the dipole moment (μ), the Boltzmann constant (k_b), and the temperature(T) [19]. The introduction of bulky groups to create free volumes and the deliberate introduction of porosity are the two main strategies to lower the dielectric constant. To our best knowledge, the introduction of trifluoromethyl group to the main chain is far more than decrease the dielectric constant. It is known that the C–F has larger bond energy than the C–C and C–O, by which the fluoropolymer has excellent heat resistance [20].

Polyarylene ether nitriles (PEN), a new type of special thermoplastic engineering plastic, its rigid aryl ether bond of molecular backbone endows superior comprehensive properties such as high temperature resistance, high flame retardancy, excellent mechanical properties [21–23]. At the

✉ Lifen Tong
tonglifen0214@163.com

✉ Xiaobo Liu
liuxb@uestc.edu.cn

[1] Research Branch of Advanced Functional Materials, School of Materials and Energy, University of Electronic Science and Technology of China, Chengdu 610054, China

same time, due to the strong polar group cyano presented on the side of the molecular, PEN possesses a good adhesion to many substances, by which can be better equipped as the insulating material for PCB [24, 25].

Since the discovery and prosperity of the fullerenes, fullerene-based materials have been convinced as photoconductors, ferromagnets, catalysts, etc. due to the unique spherical structure, physicochemical and electronic properties of fullerenes [26–29]. In our context, fullerene acts as the porogen to prepare low dielectric composites for its bulky cage structure. Despite the electrical application potential of fullerene, the well interfacial compatibility between the polymer matrix and the fullerene is still a big challenge. From big particles of 30–50 μm to the size sub-100 nm, scientists have done a lot of research on the compatibility between the fullerene and polymers [30, 31]. This problem could be tackled through mechanical introductions of fullerenes into polymers, or some methods more complicated based on chemical modification to generate fullerene derivatives and/or intermolecular complexation requiring covalent interaction [32, 33]. For example, Karsten presented an ordered structure that the thiophene-thienopyrazine oligomer was ended-capped with fullerene to cause photoinduced electron transfer reaction between the oligomer as a donor and the fullerene as a receptor, changing the electron structure of fullerene and macromolecules and consequently, changing the characteristics of the polymer matrix [34]. Compared other methods, cosolvent evaporation is the simplest solution without generating a new fullerene derivative with a high degree of complexity nor having to cope with the complex regio- and stereoselectivity during chemical modification of fullerene [35].

In our work, based on the special hollow cage structure of zero-dimensional fullerene and PEN with large substituent $–CF_3$, composite films with low dielectric constant as well as good mechanical properties were prepared by cosolvent evaporation, and the effects of different fullerene contents on the performance of the composites were discussed in detail. Moreover, taking advantage of the adhesion of the cyano group, flexible copper clad laminate was prepared by hot press successfully.

2 Experiment section

2.1 Materials

Bisphenol AF (BPAF), K_2CO_3, N-methelpyrrolidone (NMP), toluene were offered by Kelong Chemicals Ltd (Chengdu, China). 2,6-dichlorobenzonitrile (DCBN) was provided by Yangzhou Tianchen Fine Chem Co., Ltd (Yangzhou, China). All of these were analytical reagent (AR) grade and used without further purification. Fullerene (C_{60}, purity 99.9%) was purchased from Chengdu Organic Chemicals Co., Ltd (Chengdu, China).

2.2 Preparation of BPAF-PEN

The formation of polyarylene ether nitrile (PEN) is based on the nucleophilic substitution polycondensation according to the literature [22], as shown in Scheme 1. A typical PEN was synthesized by 2,6-dichlorobenzonitrile (DCBN), bisphenol AF (BPAF), together with the catalyst anhydrous K_2CO_3. First, the mixture with BPAF(0.256 mol), DCBN(0.256 mol), K_2CO_3(0.3618 mol) was added into a 500 mL three-necked bottle under stirring, which was equipped with a thermometer, a water separator, and a condenser with 150 mL NMP and 50 mL toluene. Toluene was used as dehydrating agent to get high molecule polymers. When N-methelpyrrolidone (NMP) and toluene are at the ratio of 3:1, it helps to generate the azeotrope about 150 °C, at which toluene can continuously bring out the water formed as by-product in the reaction, thus facilitating the reaction. After the reaction was carried out for 2 h, toluene was gradually discharged to raise the temperature. When the temperature rose above 180 °C, the reaction was carried out for extra 2 h until the phenomenon of climbing pole appeared. After the reaction, the product was purified and then dried in a vacuum oven at 100° C for 12 h.

2.3 Preparation of composite films

PEN/fullerene composite films were prepared by solution casting method. Fullerenes were dissolved in toluene at the concentration of 1 g L^{-1} under ultrasonic for 1 h to ensure the uniform dispersion of fullerenes. PEN was dissolved in NMP at the concentration of 0.1 g mL^{-1} under agitated stirring for 1 h to get a transparent solution. Then the PEN/fullerene mixture was obtained by adding a certain amount of fullerene solution to PEN solution. The mass ratios of fullerene/PEN are listed in Table 1. Then the toluene in mixture evaporated at 110–130° C with rapid agitation. After evaporation, the mixed solution was cast on a clean glass plate and dried in an oven with temperature programming

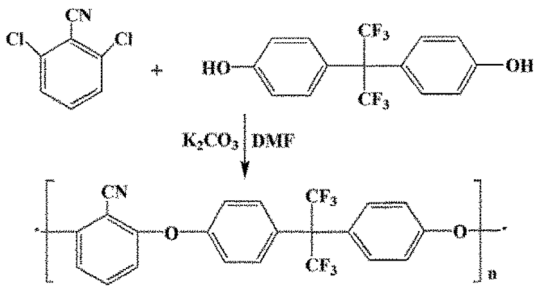

Scheme 1 Synthesis of BPAF-PEN

Table 1 The mass ratios of fullerene/PEN composite films

Samples	0 wt%	1 wt%	2 wt%	3 wt%	4 wt%
Fullerene wt%	0	1	2	3	4
BPAF-PEN wt%	100	99	98	97	96

that 80 °C (60 min), 100 °C (60 min), 120 °C (60 min), 160 °C (60 min), 200 (120 min), 220 °C (60 min) respectively. Finally, five flat composite films with approximately average thickness 60 μm were obtained.

2.4 Preparation of flexible copper clad laminate (FCCL)

The FCCL comprised of copper foil and composite films was prepared by simple hot-press without any adhesives. As shown in Fig. 1, two copper foil claddings were placed on the upper and lower sides of the composite films. They were then placed in a stainless steel mold and hot pressed at 280 °C and 10 MPa for 2 h to obtain a FCCL samples.

2.5 Characterization

The proton nuclear magnetic resonance (^{1}H NMR) spectroscopy was conducted on an NMR spectrometer (JEOL, JNMECA300, Japan) with samples dissolving in $CDCl_3$, using tetramethylsilane as the internal reference. Gel permeation chromatography (GPC) measurement was characterized on Breeze 2 HPLC system (Waters, USA) to determine the relative molecular mass and molecular mass distribution of PENs, while tetrahydrofuran was used as eluent. The morphology images of alloy composite films were collected on scanning electron microscope (JEOL, JSM-5900LV, Japan), operating at 20 kV. Films prepared for fracture surface were first quenched in liquid nitrogen at low temperature. Samples were observed after sputter-coated with gold under vacuum condition by an ion sputter (Hitachi, E-1045, Japan). Differential scanning calorimeter (DSC) studies of composite films were carried out on TA Instrument DSC Q100 equipment (New Castle, USA), at a heating rate of 10 °C min^{-1} from room temperature to 300 °C. The thermal stability of nanocomposites was investigated by Thermogravimetric analysis (TGA) using TA Instruments TGA Q50 at different heating rates (5, 10, 15, 20 °C min^{-1}) from room temperature to 600 °C under nitrogen atmosphere. Dielectric property as a function of frequency of composite films were conducted with a TH2826/A LCR meter (Tonghui Electronic Co., Ltd., China) from 100 Hz to 1 MHz. Samples were cut into roughly 10 mm × 10 mm. A thin conductive layer of silver was deposited on the both sides as an electrode to form a plate conductor. Mechanical properties were recorded on SANS CMT6104 (Shenzhen, China) series desktop electromechanical universal testing machine at room temperature. Tensile strength and tensile modulus were obtained according to the GB/T 1040.3-2006 standard test method. 180° peeling test was conducted by standard CPCA/JPCA-BM03-2005 B method experiment.

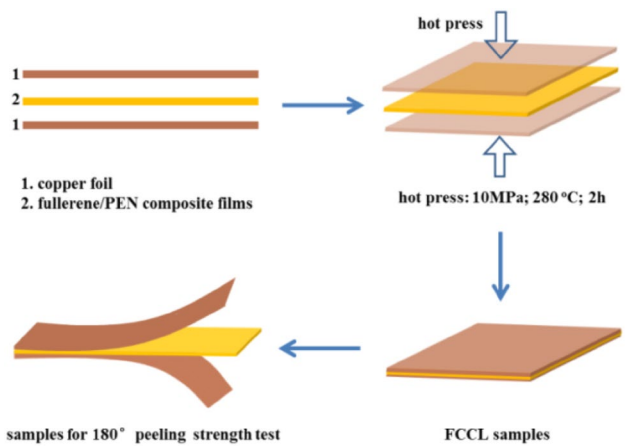

Fig. 1 Illustration of hot press for copper foil and composite films

3 Results and discussion

3.1 ^{1}H NMR

In an attempt to confirm the synthesis of the target product, ^{1}H NMR spectroscopy was used to study the chemical structure of the synthesized PEN, as shown in Fig. 2. The resonance peaks and proton numbers from the spectrum are listed as follows ($CDCl_3$, δ): 7.451–7.401 (t, 5H), 7.137–7.115, (d, 4H), 6.701–6.680 (d, 2H). The proton at the

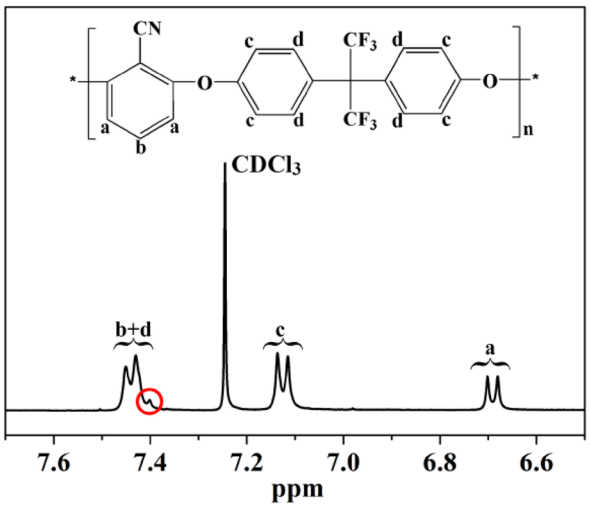

Fig. 2 ^{1}H NMR spectra of BPAF-PEN in $CDCl_3$

para-positon to the cyano group on the phenyl group shows resonance peaks around 6.701–6.680. The resonance peaks around 7.137–7.115 belong to the proton at ortho-position to ether group. In addition, it is known from the relevant reference that the peak (shown with red circle) between 7.451 and 7.401 ppm attribute to the partial overlap of the two peaks of protons b and d in the BPAF-PEN repeat unit [36]. The results reveal the successful preparation of the PEN polymer.

3.2 GPC

Molecular weight and molecular-weight distribution are two critical parameters that determine the properties of polymers [37]. The molecular weight was measured by gel permeation chromatography (GPC) using tetrahydrofuran (THF) was used as eluent. The weight-average molecular weight (M_w), number-average molecular weight (M_n) and the polydispersity index (M_w/M_n) of PEN are shown in Table 2. The M_w and M_n of PEN are 15.8×10^4 and 10.5×10^4, respectively. And the M_w/M_n is 1.50.

Table 2 Molecular mass of PEN polymers

Sample	M_w (g mol^{-1})	M_n (g mol^{-1})	PDI
BPAF-PEN	15.8×10^4	10.5×10^4	1.50

M_w weight-average molecular weight, M_n number-average molecular weight, *PDI* polydispersity index

$PDI = M_w/M_n$

3.3 SEM

To further confirm the structure of the PEN/fullerene films, high magnification scanning electron microscopy (SEM) was employed. As shown in Fig. 3a, nitrogen-induced brittle fracture surface of pure PEN film shows a relatively smooth morphology with no obvious characteristic appearance detected. While in Fig. 3b, PEN/fullerene film with 1 wt% fullerene loading has a typically uniform agglomeration of fullerenes dispersed as monodisperse clusters roughly 500 nm in diameters in the PEN matrix. The phenomenon also occurs in the other composite films with 2 wt% and 3 wt% mass fraction of fullerenes, revealing the presence of monodisperse clusters. However, when the content reaches 4 wt%, excessive globular fullerenes are incorporated, resulting in the aggregation and poor dispersion of the spherical fullerenes. All these phenomena provide the assumption for the cause of dielectric properties. It is worth mentioning that

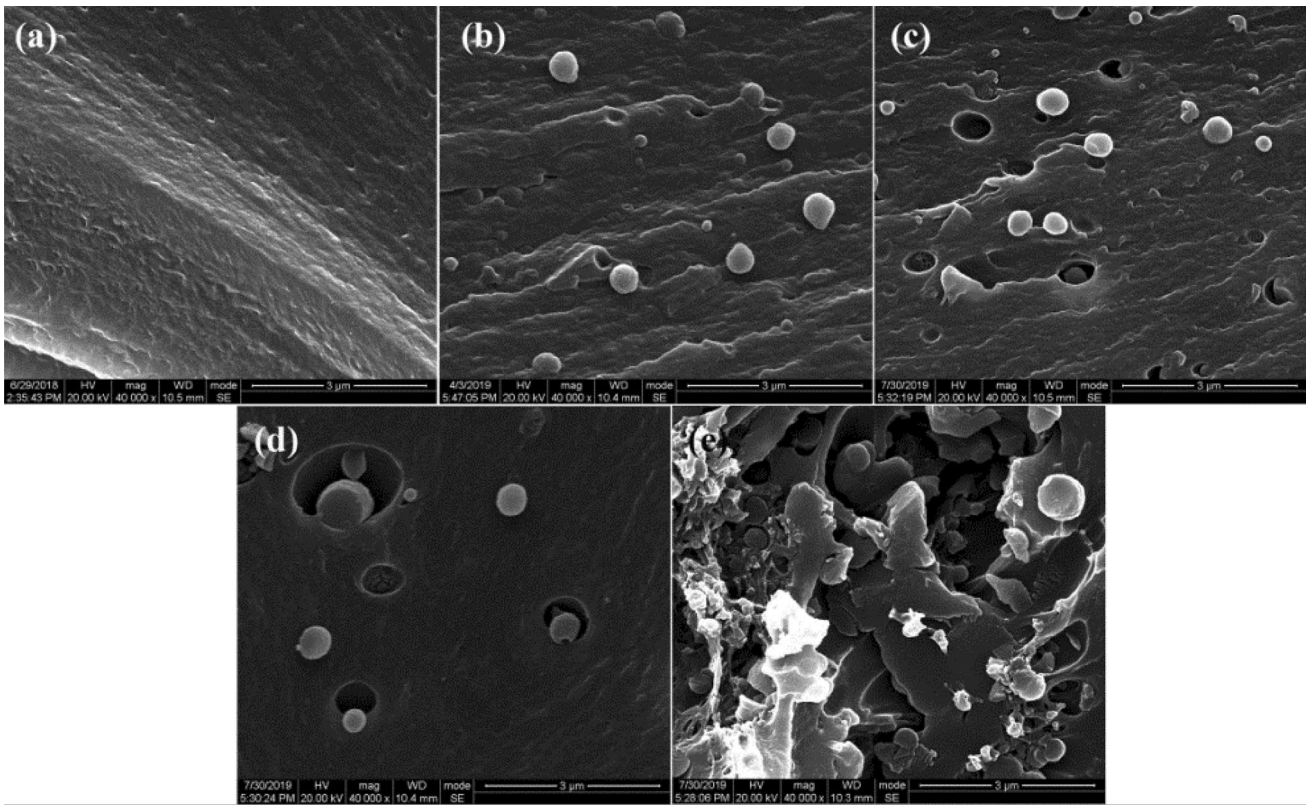

Fig. 3 SEM images of fracture surface of PEN and PEN/fullerene composite films: **a** pure PEN, **b** 1 wt% fullerene, **c** 2 wt% fullerene, **d** 3 wt% fullerene, **e** 4 wt% fullerene

fullerenes can aggregate at very low concentration, even if the concentration is only 0.78 g L^{-1} in toluene [38]. In our work, composite films with good dispersibility were produced by simple physical methods. There are two reasons for this result. First, these fullerenes are encapsulated by polymers chain and cannot be further aggregated during the stirring and distillation process. Second, it can be explained by forming organic microcrystals [39, 40]. When the concentration of fullerene reaches a saturation point, crystallization occurs and fullerene crystallites are formed.

3.4 Thermal properties

DSC and TGA curves of PEN and PEN/fullerene composite films are shown in Fig. 4. As an amorphous polymer, BPAF-PEN has a relatively low glass transition temperature (T_g) of 173 °C (Fig. 4a). Moreover, compared with the T_g of BPA-PEN (178 °C), there is a slight decrease in T_g of BPAF-PEN [22]. Since a large volume of $–CF_3$ group is introduced into the polymer, the stacking density of the molecular chain decreases and the distance between the molecular chains increases, which increases the free movement space of the polymer chain [36]. After the addition of fullerene, the T_gs of all composite films are higher than that of pure PEN. When 3 wt% fullerene is added, the T_g increases to 184 °C, and when the fullerene content continuously increases, T_g remains stable, which indicates the addition of a small amount of fullerenes can effectively inhibit the movement of PEN chains.

The TGA curves of PEN and PEN/fullerene composite films in nitrogen are presented in Fig. 4b. The corresponding characteristic thermal data are listed in Table 3 and the heat-resisting index is calculated by the equation shown below:

$$T_{\text{Heat-resistance index}} = 0.49 \times \left[T_{5\%} + 0.6 \times (T_{30\%} - T_{5\%}\right] \quad (2)$$

Table 3 TGA characteristic data of PEN and PEN/fullerene composite films

Samples	$T_{5\%}$/°C	$T_{30\%}$/°C	Heat-resistance index
0 wt%	520.73	582.92	273.44
1 wt%	524.04	589.38	275.99
2 wt%	522.53	587.50	275.14
3 wt%	522.38	584.34	274.18
4 wt%	518.45	585.69	273.81

where $T_{5\%}$ and $T_{30\%}$ is the decomposition temperature at 5% and 30% weight loss, respectively [41]. The corresponding heat-resistance index of the PEN and EN/fullerene composite films is 273.44 °C (0 wt% fullerene), 275.99 °C (1 wt% fullerene), 275.14 °C (2 wt% fullerene), 274.18 °C (3 wt% fullerene), 273.81 °C (4 wt% fullerene), respectively, as shown in Table 3. It reveals that the heat-resisting index of the PEN and PEN/fullerene composite films maintain at a relatively high value, that is, unlike the BN fillers, the incorporation of fullerenes has no significant effect on the heat resistance of PEN [42].

Studying the thermal degradation behavior of materials is of great significance to the processing and application of materials. In order to quantitatively describe the thermal stability of the composite films, the thermal degradation kinetics of 3 wt% PEN/fullerene composite films under a nitrogen atmosphere was investigated in detail by TGA. Figure 5a shows the TGA curves of 3 wt% PEN/fullerene composite films with four different heating rates in nitrogen, and the temperatures corresponding to different conversion at different heating rates are listed in Table 4, where α is conversion, β is heating rate.

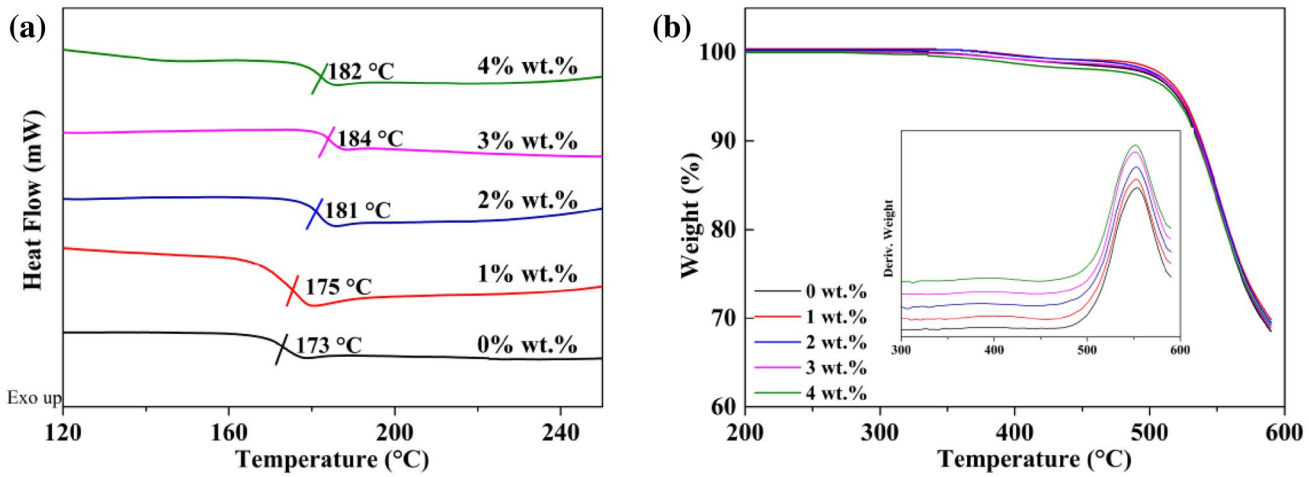

Fig. 4 DSC (**a**) and TGA (**b**) curves of PEN and PEN/fullerene composite films

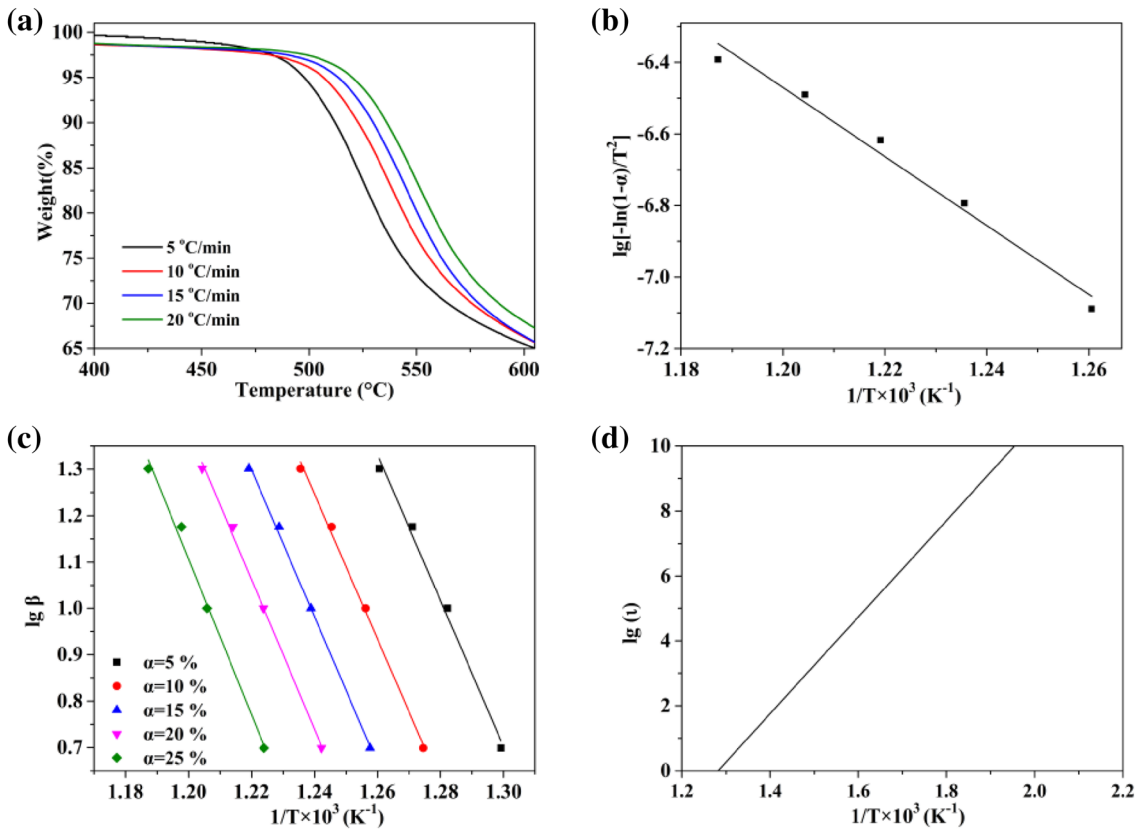

Fig. 5 **a** TGA curves for 3 wt% PEN/fullerene composite films at four heating rates in nitrogen; **b** plots of $\lg\left[-\ln(1-\alpha)/T^2\right]$ to $1/T$ by Coats-Redfern method; **c** plots of $\lg\beta$ to $1/T$ by Flynn–Wall–Ozawa method; **d** plots of $\lg\tau$ to $1/T$ by Dakin method

Table 4 The temperatures corresponding to different conversion at different heating rates

β/°C min^{-1}	α/%									
	5%		10%		15%		20%		25%	
	T/°C	$T^{-1}\times10^3$/K^{-1}	T/°C	$T^{-1}\times10^3$/K^{-1}	T/°C	$T^{-1}\times10^3$/K^{-1}	T/°C	$T^{-1}\times10^3$/K^{-1}	T/°C	$T^{-1}\times10^3$/K^{-1}
5	496.56	1.299	511.46	1.275	522.01	1.258	531.86	1.242	543.88	1.224
10	506.73	1.282	522.89	1.256	534.06	1.239	543.99	1.224	556.10	1.206
15	513.56	1.271	529.78	1.245	540.71	1.229	550.51	1.214	561.75	1.198
20	520.15	1.261	536.19	1.236	547.12	1.219	557.19	1.204	569.14	1.187

An integral method developed by Coats and Redfern [Eq. (3)] can be applied to obtain the correct reaction order, n [43], where T is the absolute temperature, A is the pre-exponential factor, R is the universal gas constant, and E_a is the activation energy. Assuming that the reaction is a first order reaction, $g(\alpha) = -\ln(1-\alpha)$. In this paper, β=20 °C min^{-1} in Tale 4 is selected to plot $\lg\left[-\ln(1-\alpha)/T^2\right]$ to $1/T$. The result is shown in Fig. 5b. It can be seen that the curve has a good linear relationship, indicating that the thermal degradation of the 3 wt% PEN/fullerene composite films is a first order reaction. Moreover, various approximations lead to Flynn–Wall–Ozawa isoconversional methods [43], Eq. (4), a thermal degradation kinetic model for multi-carbon polymers. Plot lnβ to $1/T$, linearly fit to get straight lines with a slope of $0.4567E_a/R$ has been shown in Fig. 5c, so that the reaction activation energy E_a and pre-exponential factor A can be obtained and listed in Table 5.

$$\lg\left[\frac{g(\alpha)}{T^2}\right] = \lg\left[\frac{AR}{\beta E_a}\left(1-\frac{2RT}{E_a}\right)\right] - \frac{E_a}{2.303RT} \tag{3}$$

$$\lg\beta = \lg\frac{AE_a}{-R\ln(1-\alpha)} - 2.31 - 0.4567\frac{E_a}{RT} \tag{4}$$

Table 5 Kinetic parameters obtained using Flynn–Wall–Ozawa

α/%	Slope	E_a/kJmol^{-1}	Intercept	A/min^{-1}
5	− 16.79	305.45	21.24	5.02×10^7
10	− 16.13	293.65	20.74	3.40×10^7
15	− 15.84	288.39	20.63	4.08×10^7
20	− 15.64	284.65	20.64	5.81×10^7
25	− 15.75	286.74	21.18	25.97×10^7

The observed deterioration at high temperatures during thermal aging is the result of thermal degradation reaction. Dakin [44] proposed an empirical formula to predict the life of the materials. Its integral form is shown by Eq. (5), where τ is the lifetime of the composite films at temperature T, $\alpha\tau$ is percent residual at end point. From what we have discussed above, n is determined to be 1. When n = 1, Eq. (5) can be transformed into Eq. (6). $E_a = 284.65$ kJ mol^{-1} and $A = 25.97\times10^{17}$ min^{-1} in Table 5 was used and the weight loss of 5% was taken as the end point. Then, the straight line with the slope of 14.87×10^3 and intercept of − 19.05 was drawn in Fig. 5d, where the lifetime of the 3 wt% PEN/fullerene composite films at different temperature or the ultimate service temperature at different aging life can be estimated. Therefore, at the temperature of 300 °C, the expected service life of the 3 wt% PEN/fullerene composite films to reach 5 percent weight loss would be about 3.3 years, under the condition of nitrogen filled atmosphere.

$$\int_1^{\alpha\tau} -\frac{d\alpha}{\alpha^n} = A\exp\left(-\frac{E}{RT}\right)\int_0^{\tau} dt \tag{5}$$

$$\lg\tau = \frac{E_a}{2.303RT} + \lg\left(\frac{-\ln\alpha\tau}{A}\right) \tag{6}$$

3.5 Dielectric properties

The values of the dielectric constant and the dielectric loss of composite films are the key parameters in designing novel and advanced functional materials for technological applications such as flexible organic electronics. Hence, the dielectric properties of the PEN/fullerene films were investigated at room temperature in the frequency range from 100 Hz to 1 MHz. Before test, samples were dried at 110 °C for 1 h to prevent the inherently high dielectric constant of water, 80. As can be seen from Fig. 6a, b, by adding the pores structure, the composite films with fullerenes show a significant decrease in the dielectric constant and dielectric loss. At the frequency of 1 MHz, the dielectric constant decreases from 3.13 (pure PEN) to 2.65 when the load of the fullerene is 3 wt% (Fig. 6c), and the dielectric loss decreases from 0.007 to 0.005 (Fig. 6b). Meanwhile, the dielectric constant of all PEN/fullerene composite films remains stable in the range of 100 Hz to 1 MHz and shows low frequency dependence. It is shown that the incorporation of fullerenes in the polymer matrix will result in a decrease in dielectric constant. The dielectric constant of air is 1.0, so the air voids stored in the spherical fullerenes are the main cause of a decrease in dielectric constants. There are also some air voids in the gaps on the interfaces between the spherical fullerenes and the PEN matrix (Fig. 3). Therefore, the decrease of the dielectric constant is contributed by the whole air voids created by incorporating the spherical fullerenes, including the air volume stored within the spherical fullerenes, the air voids come from the gaps on the interfaces between the spherical fullerenes and the PEN matrix [45]. On the contrary, when the content reaches 4 wt%, excessive globular fullerenes are incorporated, resulting in the aggregation and poor dispersion of the spherical fullerenes, as can be seen in Fig. 3e, which in turn lead to the stable increment of the dielectric constant. Moreover, the dielectric constant of pure BPAF-PEN is 3.13 at 1 kHz, which is notably lower than BPA-PEN, 3.51 at 1 kHz [22]. The result suggests that the introduction of large volume of fluorine-containing substituent is an effective way to lower the dielectric constant of PEN.

3.6 Mechanical properties

Mechanical property is also an important factor for the application of the low-k materials. In this part, the mechanical properties of the PEN/fullerene composite films were analyzed with the tensile tests. Porous structure introduced into the matric by physical or chemical methods are always responsible for plenty of manufacturing issues, such as the effect of moisture and the mechanical properties [19]. Figure 7 shows the mechanical properties of pure PEN and PEN/fullerene composite films. Surprisingly, the tensile strength and tensile modulus tend to be stable and fluctuate in the range of 92 ± 2 MPa and 2594 ± 132 MPa. The study demonstrates that the introduction of fullerenes with a cage structure as a porogen does not degrade the mechanical properties of PEN. As is known to all, the mechanical performances of the polymer-based nanocomposites depend on the filler dispersion and interfacial interaction [34]. On one hand, with the gaps between the fullerene clusters and the PEN matrix, the tensile strength decreases. On the other hand, the mobility of the matrix is restricted by the fullerene clusters uniformly dispersed in the PEN matrix, which can improve the tensile strength and tensile modulus. Both actions are carried out simultaneously, keeping the mechanical properties stable over a low concentration range.

3.7 Application

PEN offers great potential for FCCL with high temperature resistance and high signal transmission efficiency that

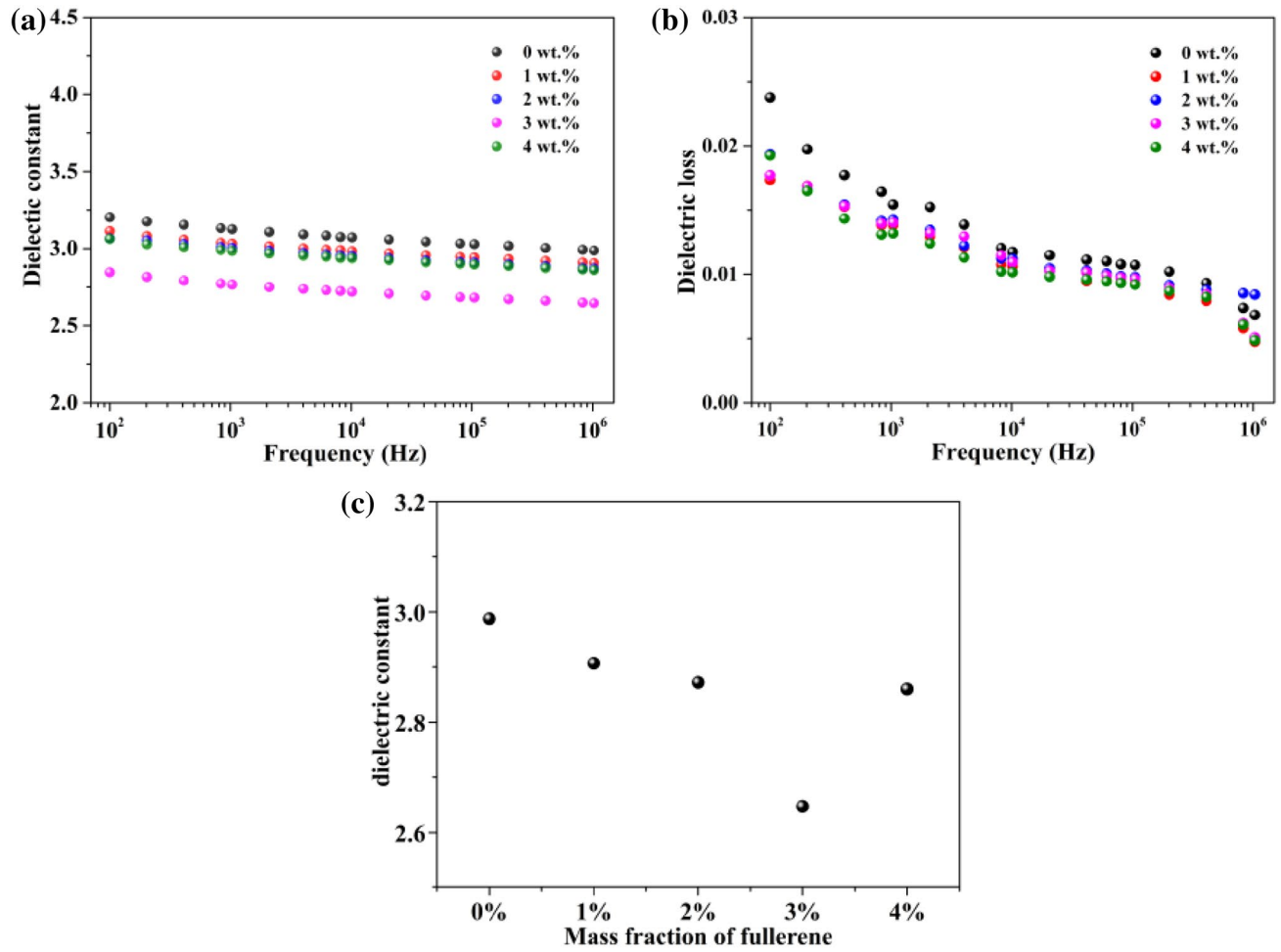

Fig. 6 Relationships between dielectric properties and frequency of PEN and PEN/fullerene composite films: **a** dielectric constant, **b** dielectric loss; **c** relationship between dielectric constant and mass fraction of fullerene in PEN/fullerene composite films at 1 MHz

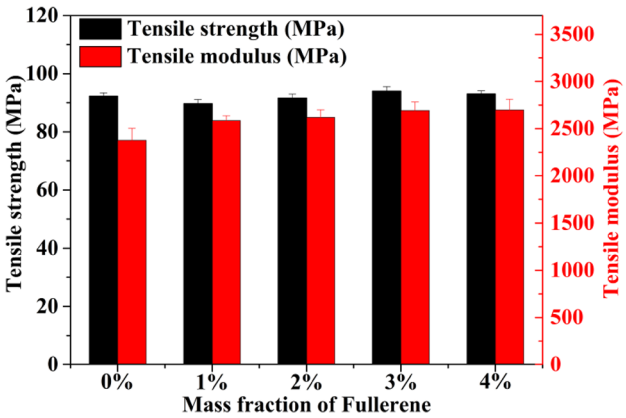

Fig. 7 Mechanical properties of PEN and PEN/fullerene composite films

is expected to be suitable for 5G materials. 3 wt% PEN/fullerene composite film was chosen to prepare FCCL by hot pressing method due to its lower dielectric constant (Fig. 8), and the hot pressing process is shown in Fig. 1. The 180° peeling test was used to investigate whether it can be applied in industry. Films exhibited better adhesion to copper foil with the peeling strength higher than 6.91 N cm^{-1}, compared with the previous study, 1.52 N cm^{-1} [46], which because of the cyano group on the main chain of the PEN [24, 25].

4 Conclusions

In summary, we report a novel composite with low dielectric constant by introducing fullerenes into BPAF-PEN through cosolvent evaporation, which is the easiest method to obtain PEN/fullerene composite films with well-defined monodisperse fullerene clusters. The DSC analysis indicates that the T_g of 3 wt% PEN/fullerene composite films is highest. The

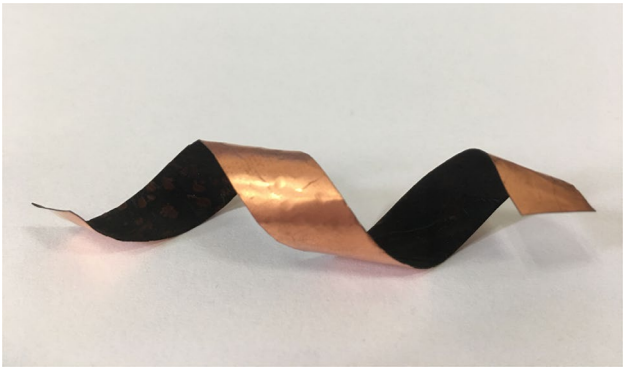

Fig. 8 The picture of FCCL

thermodynamic calculation shows that the composite film containing 3 wt% fullerene has a predicted service life for 3.3 years reaching a weight loss of 5% at 300 °C in nitrogen. And 3 wt% PEN/fullerene composite films has the lowest dielectric constant 2.65 at 1 MHz basically meet the requirements for use in industry. The application of composite films to FCCL is worth noting that the 180° peeling strength of the 3 wt% PEN/fullerene composite film and copper matrix is 6.91 N cm^{-1} without any adhesive. This study demonstrates the importance of trifluoromethyl group and bulky cage structure in lower the dielectric constant.

Acknowledgements The financial supports from the National Natural Science Foundation of China (51603029, 51773028 and 51903029), China Postdoctoral Science Foundation (2017M623001) and National Postdoctoral Program for Innovative Talents (BX201700044) are gratefully acknowledged.

References

1. H. Zuo, S. He, IEEE Trans. Ind. Electron. **63**, 3009 (2016)
2. T. Aizawa, K. Okagawa, M. Kashani, J. Mater. Process. Technol. **213**, 1095 (2013)
3. J.-W. Yoon, J.-G. Lee, J.-B. Lee, B.-I. Noh, S.-B. Jung, J. Mater. Sci. **23**, 41 (2012)
4. K. Devendra, T. Rangaswamy, J. Miner. Mater. Charact. Eng. **1**, 353 (2013)
5. R.K. Goyal, A.N. Tiwari, Y.S. Negi, Compos. B **47**, 70 (2013)
6. R.K. Goyal, K.A. Rokade, A.S. Kapadia, B.S. Selukar, B. Garnaik, Electron. Mater. Lett. **9**, 95 (2013)
7. A.M. Patki, R.K. Goyal, J. Mater. Sci. **30**, 3899 (2019)
8. N. Kränzlin, S. Ellenbroek, D. Durán-Martín, M. Niederberger, Angew. Chem. Int. Ed. **51**, 4743 (2012)
9. D. Paeng, J.H. Yoo, J. Yeo, D. Lee, E. Kim, S.H. Ko, C.P. Grigoropoulos, Adv. Mater. **27**, 2762 (2015)
10. W.H. Chung, H.J. Hwang, H.S. Kim, Thin Solid Films **580**, 61 (2015)
11. A. Bag, S.H. Choi, Mater. Charact. **129**, 186 (2017)
12. J.B. You, S.Y. Kim, Y.J. Park, Y.G. Ko, S.G. Im, Langmuir **30**, 916 (2014)
13. METIS, (In: EU 7th Framework Programme Project. 2013) https://www.metis2020.com. Accessed 26 May 2019
14. P.A. Kohl, Annu. Rev. Chem. Biomol. Eng. **2**, 379 (2011)
15. C. Yuan, K.K. Jin, K. Li, S. Diao, J. Tong, Q. Fang, Adv. Mater. **25**, 4875 (2013)
16. C. Yuan, J. Wang, K.K. Jin, S. Diao, J. Sun, J. Tong, Q. Fang, Macromolecules **47**, 6311 (2014)
17. L.K. Lin, C.C. Hu, W.C. Su, Y.L. Liu, Chem. Commun. **51**, 12760 (2015)
18. L. Tong, X.T. Lei, G.Y. Yang, X.B. Liu, Polymers **11**, 1403 (2019)
19. W. Volksen, R.D. Miller, G. Dubois, Chem. Rev. **110**, 56 (2010)
20. P. Yao, J. Gu, X. Lei, W. Sun, Y. Chen, Q. Zhang, J. Appl. Polym. Sci. **132**, 41713 (2015)
21. R. Wei, L. Tu, Y. You, C. Zhan, Y. Wang, X. Liu, Polymer **161**, 162 (2019)
22. H. Tang, J. Yang, J. Zhong, R. Zhao, X. Liu, Mater. Lett. **65**, 2758 (2011)
23. Y. Lei, Z. Han, D. Ren, H. Pan, M. Xu, X. Liu, Macromol. Res. **26**, 602 (2018)
24. C. Li, X. Liu, Mater. Lett. **61**, 2239 (2007)
25. Y. Zhan, F. Meng, X. Yang, X. Liu, Colloids Surf. A **390**, 112 (2011)
26. H.W. Kroto, J.R. Heath, S.C. O'Brien, R.F. Curl, R.E. Smalley, Nature **318**, 162 (1985)
27. J. Benduhn, K. Tvingstedt, F. Piersimoni et al., Nat. Energy **2**, 17053 (2017)
28. H. Khalatbari, S.I. Vishkayi, H.R. Soleimani, Physica E **108**, 372 (2019)
29. F. Gao, G.L. Zhao, S. Yang, J.J. Spivey, J. Am. Chem. Soc. **135**, 3315 (2013)
30. C.J. Brabec, V. Dyakonov, N.S. Sariciftci, J. Chem. Phys. **109**, 1185 (1998)
31. J.F.R.V. Guyse, V.R. Rosa, R. Lund, M.D. Bruyne, R.D. Rycke, S.K. Filippov, R. Hoogenboom, ACS Macro Lett. **8**, 172 (2019)
32. E. Badamshina, M. Gafurova, J. Mater. Chem. **22**, 9427 (2012)
33. E.R. Badamshina, M.P. Gafurova, Polym. Sci. B **49**, 182 (2007)
34. B.P. Karsten, R.K.M. Bouwer, J.C. Hummelen, R.M. Williams, R.A.J. Janssen, J. Phys. Chem. B **114**, 14149 (2010)
35. K.N. Semenov, N.A. Charykov, V.N. Keskinov, J. Chem. Eng. Data **56**, 230 (2011)
36. J. Wei, X. Meng, X. Chen et al., J. Appl. Polym. Sci. **135**, 46837 (2018)
37. Y. You, S.N. Liu, L. Tu, Y.J. Wang, C.H. Zhan, X.Y. Du, R. Wei, X.B. Liu, Macromolecules **52**, 5850 (2019)
38. L.A. Bulavin, I.I. Adamenko, V.M. Yashchuk, T.Y. Ogul'chansky, Y.I. Prylutskyy, S.S. Durov, P. Scharff, J. Mol. Liq. **93**, 187 (2001)
39. A.J. Moulé, K. Meerholz, Adv. Mater. **20**, 240 (2008)
40. K. Hitoshi, O. Hidetoshi, O. Shuji, N. Hachiro, Bull. Chem. Soc. Jpn **71**, 2597 (1998)
41. J. Gu, Y. Guo, Z. Lv, W. Geng, Q. Zhang, Compos. A **78**, 95 (2015)
42. X.T. Yang, Y.Q. Guo, X. Luo et al., Compos. Sci. Technol. **164**, 59 (2018)
43. T. Ozawa, Bull. Chem. Soc. Jpn. **38**, 1881 (1965)
44. T.W. Dakin, Trans. Am. Inst. Electron. Eng. **67**, 113 (1948)
45. Y. Yuan, B.P. Lin, Y. Sun, J. Appl. Polym. Sci. **120**, 1133 (2010)
46. K. Li, L. Tong, K. Jia, X. Liu, J. Mater. Sci. **25**, 5446 (2014)